Synthesis, crystal structure, and electrical and magnetic characterizations of the monoclinic compounds Ln3Mo4+xSi1-xO14 (Ln = La, Ce, Pr, and Nd; X = 0 and 0.35) containing Mo3 clusters and Mo2 dimers

Patrick Gougeon, Philippe Gall

Synthesis, crystal structure, and electrical and magnetic characterizations of the monoclinic compounds $Ln_3Mo_{4+x}Si_{1-x}O_{14}$ (Ln = La, Ce, Pr, and Nd; X = 0 and 0.35) containing Mo_3 clusters and Mo_2 dimers

Philippe Gall[†], and Patrick Gougeon[*]

Institut des Sciences Chimiques de Rennes, UMR 6226 CNRS – Université de Rennes 1 – INSA de Rennes, 11 allée de Beaulieu, CS 50837, 35708 Rennes Cedex, France

.

*Corresponding author : patrick.gougeon@univ-rennes1.fr
Tel : + 33 2 23 23 62 54
Fax : + 33 2 23 23 67 99

Abstract

Powder samples of the new monoclinic compounds $Ln_3Mo_4SiO_{14}$ (Ln = La, Ce, Pr and Nd) and single crystals of $Pr_3Mo_{4.35}Si_{0.65}O_{14}$ were obtained by solid state reaction. The crystal structure of $Pr_3Mo_{4.35}Si_{0.65}O_{14}$ was determined by single-crystal X-ray diffraction. $Pr_3Mo_{4.35}Si_{0.65}O_{14}$ crystallizes in the monoclinic space group $P2_1/n$ with unit-cell parameters a = 5.6361 (2) Å, b = 17.5814 (8) Å, c = 10.9883 (4) Å and Z = 4. Full-matrix least-squares refinement on F^2 using 7544 independent reflections for 203 refinable parameters results in R_1 = 0.0359 and wR_2 = 0.0831. The structure contains chains of Mo_3O_{13} clusters and chains of edge-sharing MoO_6 octahedra with alternately short (2.508 Å) and long (3.162 Å) Mo-Mo distances running parallel to the *a* axis that are separated by eight- or ten-coordinate Pr-O polyhedra. Magnetic susceptibility measurements on the $Ln_3Mo_4SiO_{14}$ (Ln = La, Ce, Pr and Nd) are in agreement with a trivalent state of the rare earths for the Ce, Pr and Nd compounds, while that on the lanthanum compound confirm the presence of one unpaired electron per Mo_3 as expected. Resistivity measurements on a single crystal show that $Pr_3Mo_{4.35}Si_{0.65}O_{14}$ is a small band gap semi-conductor.

Keywords

Mo cluster oxides, MoO_2 type chains, Mo_3 triangle, rare earth, magnetic susceptibility properties, resistivity measurement.

Introduction

The triangular Mo_3 cluster has been observed for the first time in solid state chemistry in the series $M_2Mo_3O_8$ (M = Mg, Mn, Fe, Co, Ni, Zn and Cd) synthesized by McCarroll et al. in 1957 [1]. During the last decade, such compounds containing Mo_3 triangle clusters have experienced a resurgence of interest both in terms of purely fundamental studies as well as for their potential applications. Owing to their non-centrosymmetric polar crystal structure (space group $P6_3mc$), the $M_2Mo_3O_8$ (M = Mn, Fe, Co and Ni) compounds become multiferroics with very important magneto-electric coupling. Among the latter compounds, $Fe_2Mo_3O_8$ has been particularly studied [2-7]. Thus, a large tunable magnetoelectric effect [3, 4, 6] as well as an optical diode effect [5] have been observed in Zn-doped $Fe_2Mo_3O_8$. A very large thermal Hall effect has been also measured on crystals of the solid solution $(Fe_{1-x}Zn_x)_2Mo_3O_8$ [7], showing for the first time the coupling between magnetism and phonon in thermal transport properties. $Fe_2Mo_3O_8$ either alone or with graphene oxide or reduced graphene oxides has also been studied for Li storage in batteries [8, 9]. The cluster magnet $LiZn_2Mo_3O_8$ compound has also been the subject of very interesting studies by the group of T. M. McQueen [10-13]

In the 1980s, McCarroll reported the crystal structures of the isomorphous orthorhombic $La_3Mo_4XO_{14}$ (X = Si or $Mo_{0.33}Al_{0.67}$) compounds [14, 15]. Both compounds were prepared by electrolytic reduction at 1373 K of melts containing Na_2MoO_4, MoO_3, and La_2O_3 in silica or alumina crucibles. The composition of the crystals which grown at the platinum cathode depends upon the type of crucible used to contain the melt. Indeed, the silica crucible produces $La_3Mo_4SiO_{14}$ while the alumina crucible yields $La_3Mo_4(Mo_{0.33}Al_{0.67})O_{14}$. The crystal structure of the latter two compounds contains triangular Mo_3O_{13} cluster units with Mo-Mo distances of about 2.56 Å and chains of edge-sharing MoO_6 octahedral with alternately short (ca. 2.53 Å) and long (ca. 3.16 Å) Mo-Mo distances. The Si and the Al and Mo atoms are tetrahedrally

coordinated and the La atoms are surrounding by 7, 8 or 10 O atoms forming bi-, tri- or tetra-capped distorted trigonal prisms

We present here the crystal structure of $Pr_3Mo_{4.35}Si_{0.65}O_{14}$ which constitutes a monoclinic variant of the $La_3Mo_4XO_{14}$ structure-type. Similarly, to the previous compounds, $Pr_3Mo_{4.35}Si_{0.65}O_{14}$ was obtained serendipitously by solid-state reaction. As for $La_3Mo_4SiO_{14}$, Si was abstracted from the silica tube used to contain the reactants since the starting products were Pr_6O_{11}, Gd_2O_3, MoO_3, and Mo. Subsequently, we have prepared, by solid state reaction, polycrystalline samples of the monoclinic series $Ln_3Mo_4SiO_{14}$ (X = La, Ce, Pr and Nd). Synthesis, and electrical resistivity and magnetic susceptibility measurements of the latter compounds are also presented in this paper.

1. Experimental

2.1 *Syntheses*

Some poor quality crystals of the monoclinic $Pr_3Mo_{4.35}Si_{0.65}O_{14}$ compound were obtained serendipitously during the synthesis of Pr_3MoO_7 by solid-state reaction in sealed silica tube at 1200 °C. As for the orthorhombic $La_3Mo_4SiO_{14}$ compound synthesized by fused salt electrolysis, Si was abstracted from the silica tube used to contain the reactants. Crystals thus obtained have the shape of needles with quasi-rectangular cross-section. Qualitative microanalyses using a JEOL JSM 6400 scanning electron microscope equipped with an OXFORD link INCA energy-dispersive- X-ray analyser confirmed the presence of silicon in the crystals. Subsequently, powders of the monoclinic $Ln_3Mo_4SiO_{14}$ (Ln = La, Ce, Pr and Nd)

compounds were prepared from stoichiometric mixtures of the rare-earth oxides (La_2O_3, CeO_2, Pr_6O_{11} or Nd_2O_3), MoO_3 and Mo. Prior reactions, the molybdenum powder was heated at 1000°C under a H_2 flow during 6 hours. The rare-earth oxides were heated at 1000° C during 12 hours and after, left at 800°C before syntheses. After homogenization, the powders were pelletized (approximately 5 g) and introduced into Mo crucibles, which were degassed beforehand at temperatures of approximately 1500 ° C for 15 min under a dynamic vacuum of approximately 10^{-2} Pa. The Mo crucibles were then sealed under an Ar pression of about 60 Pa by arc welding. The samples were subsequently heated to the temperature of 1300°C with a rate of rise of 300°C/h. The duration of the plateau at 1300°C was 48 hours and then the whole was subsequently cooled to 1100 ° C at the rate of 100 °C/h, temperature at which the oven was stopped and cooled itself down to room temperature. The microcrystalline powder samples, thus obtained, were found to be monophasic based on their X-ray diffraction diagram collected on a Bruker D8 advance diffractometer equipped with a LynxEye detector ($CuK\alpha_1$ radiation) and indexed in a monoclinic unit cell as exemplified by that of $Pr_3Mo_4SiO_{14}$ in Figure 1. The lowering of the orthorhombic symmetry of the unit-cell to monoclinic results in splitting of some peaks as exemplified by the (101) and (111) reflections in Figure 2. Unit cell parameters of the $Ln_3Mo_4SiO_{14}$ compounds determined by profile matching fits with the program JANA2006 [16] in the space group $P2_1/n$ are given in table 1. Figure 3 shows a decrease of the unit-cell volume from the La to the Nd compound. This behaviour is in agreement with the well-known lanthanide contraction very often observed in the series of lanthanide-based compounds and confirms that all rare earths are in a trivalent state in our phases. Attempts to grow single crystals of the monoclinic $Ln_3Mo_4SiO_{14}$ (Ln = La, Ce, Pr and Nd) compounds by a solid-state procedure were unsuccessful up to now.

2.2 *Single-crystal study*

Several crystals of $Pr_3Mo_{4.35}Si_{0.65}O_{14}$ were tested on a Nonius Kappa CCD diffractometer using graphite-monochromated Mo-Kα radiation (λ = 0.71073 Å). All of them were of poor quality, and present a substantial mosaic spread due to a twinning. Nevertheless, the totality of the reflections was identified with a primitive monoclinic unit-cell after introducing a twinning matrix corresponding to a twofold rotation about the c axis. The COLLECT program [17] was employed to determine the angular scan conditions (φ and ω scans) for the intensity recording. The raw data were subsequently integrated with the package EvalCCD [18]. The analytical method as developed by de Meulenaar and Tompa was employed for the correction of the absorption after the indexation of the faces of the crystal investigated [19]. Analysis of the intensity data shows that the reflections (h0l) with h +l = 2n + 1 as well as (0k0) k = 2n+1 were systematically absent, leading to the monoclinic space group $P2_1/n$. The crystal structure was solved by direct methods using the software SIR97 [20] and subsequently refined with SHELXL97 [21] in the monoclinic $P2_1/n$ space group. Analysis of the data with the TwinRotMat procedure implemented in PLATON [22] confirmed that the crystal investigated was twinned with the two crystalline components related by a [001] twofold axis. Experimental crystal data and structure refinement results for $Pr_3Mo_{4.35}Si_{0.65}O_{14}$ are recapitulated in Table 2, and the principal interatomic bond lengths are given in Table 3

2.3 *Electrical Resistivity Study*

The electrical resistivity measurements were realized on a single crystal of $Pr_3Mo_{4.34}Si_{0.66}O_{14}$ with an ac current of 1 μA and a frequency of 80 Hz using the classical four-probe method. The four indium contacts were attached to the crystal by an ultrasonic soldering iron.

2.4 *Magnetic susceptibility characterizations*

Magnetic susceptibility measurements were made on microcrystalline powder samples of about 100 mg on a *MPMS XL* Magnetometer from Quantum Design in the temperature range 4.2 - 300 K and under a magnetic field of 0.5 T.

2. Results and discussion

3.1 *Crystal structure*

The figure 4 represent a projected view of the crystal structure of $Pr_3Mo_{4.35}Si_{0.65}O_{14}$ along the a axis. The Mo-O network is similar to that of the orthorhombic $La_3Mo_4XO_{14}$ compounds. It is based on chains of the well-known triangular Mo_3O_{13} unit (Fig. 3) and chains of MoO_6 octahedra of rutile-type as observed in the molybdenum dioxide MoO_2 [23]. Each rutile type Mo chain is connected via the oxygen atoms O4 and O9 to two chains made up of Mo_3 triangles to create a kind of ribbon, which develops along the b axis (fig.2). The most important difference between the orthorhombic and monoclinic variants arises from the loss of the mirror plane perpendicular to the smallest axis. Indeed, in the orthorhombic phase, it was necessary to move off the mirror plane the unique crystallographically Mo atom forming the edge sharing MoO_6 chains with a site occupancy factor of 0.5 to describe the alternately long and short Mo-Mo distances encountered in this MoO_2-type chain. In the monoclinic compound, such an arrangement could be accommodated without disorder with one Mo atom, Mo4, in general position. The Mo-Mo distances along the chain are 2.5083(7) and 3.1609(7) Å in the monoclinic compound compared to 2.535(8) and 3.167(8) Å in the previous orthorhombic compounds. In the trimer Mo_3, the three Mo-Mo bond lengths are 2.5400(6), 2.5455(6) and 2.5584(4) Å leading to an average value of 2.548 Å in the range 2.47-2.58 Å of what is observed in the Mo_3 triangles found in the reduced molybdenum oxides containing such units. The absence of the mirror plane also reduces the symmetry of the Mo_3O_{13} unit as well as that of the rare-earth sites from .m. to 1. The Mo-O bond lengths around the Mo1, Mo2 and Mo3 atoms of the Mo_3 cluster

are in the range 1.928(4) - 2.132(4) Å compared to 1.918(3) - 2.107(4) Å around the Mo4 atoms of the Mo_2 dimer. From the lengths of the Mo-O bonds, we were able to obtain an estimate of the oxidation state of each independent Mo atom from the bond-length bond-strength equation, $s(Mo\text{-}O) = [d(Mo\text{-}O)/1.882]^{-6}$, established by Brown and Wu [24]. In this formula, s(Mo-O) is the bond strength in valence unit, d(Mo-O) the observed Mo-O bond distance in Å, 1.882 Å corresponds to a Mo-O single bond distance and the exponential parameter -6 is characteristic of the Mo atom. Consequently, for the Mo1, Mo2 and Mo3 atoms forming the Mo_3 cluster, the values of +4.03(5), +3.49(5) and +3.71(5) were obtained, and for Mo4 of the MoO_2-type chain we got +3.77(4). Consequently, the average valence for the Mo atoms of the Mo_3 clusters is +3.74, and +3.77 for the Mo atoms belonging to the MoO_2-type chains. From these two values, we can deduce value of 6.8 e^-/Mo3 and 3.8 e^-/Mo2 in good agreement with the expected value of 7 e^-/Mo3 and 4 e^-/Mo2 deduced from the formula. For the orthorhombic $La_3Mo_4SiO_{14}$, quasi-similar calculated values of +3.76 and +3.84 are found while in $La_3Mo_4Al_{2/3}Mo_{1/3}O_{14}$, they slightly differ due the trivalent state of the aluminium with values of +3.90 for the Mo_3 cluster and +3.93 for those in the MoO_2-type chains. In table 4, we have summarized the number of electrons per Mo_3 cluster deduced from stoichiometry and from the Brown and Wu relationship for compounds containing Mo_3 clusters the crystal structures of which were determined on single crystals. These calculations of bond valences have been used with success in numerous reduced molybdenum containing various Mo clusters and chains for many years. As we can, there is no correlation between the number of electrons bears by the triangular cluster and the distances between the atoms of molybdenum that form it. This is particularly highlighted with the compounds having clusters with 8 electrons and in which the Mo-Mo distances vary from one extreme to the other indicating that matrix effects are more important than electronic ones.

In $Pr_3Mo_{4.35}Si_{0.65}O_{14}$, the Si atom is tetrahedrally coordinated by O atoms with Si-O distance ranging from 1.460(5) to 1.750(5) Å. The relationship of Brown and Wu was also applied to

the Si-O bonds ($s = [d(Si-O)/1.622]^{-4.429}$). The oxidation state of +4 for the Si atoms was confirmed with a calculated value of +3.9.

The Pr atoms are surrounded by 7, 8 or 10 oxygen atoms forming complex polyhedral based, in each case, on a trigonal prism of oxygen atoms. For the atoms Pr3 and Pr1, one or two pseudo-rectangular faces are capped, respectively, and, for Pr2, the two distorted triangular faces are also capped. In these three sites, the Pr-O distances range from 2.334(5) to 2.936(6) Å with average distances of 2.50 Å for the Pr1 and Pr3 sites (coordination number (CN) 8 and 7, respectively) and 2.63 Å for the Pr2 site (CN 10). The latter values compare well with those deduced from the sum of the ionic radii of O^{2-} and Pr^{3+} reported by Shannon, respectively 2.52 Å for the Pr1 and Pr3 sites and 2.56 Å for the Pr2 site [34]. From the bond length-bond strength formula, the oxidation states of +3.16, +2.91 and +2.70 were calculated for the Pr1, Pr2 and Pr3 atoms, respectively (average value +2.93).

3.2 *Electrical and magnetic characterizations*

Electrical resistivity measurements were performed on a single-crystal of $Pr_3Mo_{4.35}Si_{0.65}O_{14}$. The thermal variation of the electrical resistivity was measured along the a axis corresponding to the direction of propagation of the cluster chains. $Pr_3Mo_{4.35}Si_{0.65}O_{14}$ presents a semiconductor behaviour between 100 and 290 K as depicted by the curves shown in figure 8 that represent the thermal variation of the resistivity and log(ρ) as a function of 1000/T. The resistivity measured at 290K is 0.6 Ω.cm and the activation energies deduced from the Arrhenius plot is 0.06 eV. Those values agree well with those published by Betteridge et al. in 1984 and McCarroll et al. in 1986 for the orthorhombic variants with room temperature resistivities in the range 0.2 - 0.9 Ω.cm and activation energies around 0.05 eV.

The reciprocal magnetic susceptibility of $La_3Mo_4SiO_{14}$ as a function of the temperature is shown in Fig. 9. Above 150 K, the curve of the reciprocal magnetic susceptibility as a function of the temperature follows a modified Curie-Weiss law that could fitted with a constant of Curie C = 0.248 leading to a magnetic moment of 1.41 μ_B per Mo_3 cluster if we assume that no magnetic moment arises from the MoO_2 rutile-type chains. The latter value, lower than the expected one of 1.73 μ_B for a single unpaired spin, confirms a configuration of seven electrons on each Mo_3 clusters in $La_3Mo_4SiO_{14}$. The experimental magnetic moments observe for the reduced molybdenum oxides with non-magnetic cations based on triangular Mo_3 clusters having 7 electrons are given in table 5. Chen et al. [35] introduce a phenomenological parameter λ to characterize the anisotropy of the Mo Kagome lattice such that $\lambda = d(Mo\text{-}Mo)_{inter}/d(Mo\text{-}Mo)_{intra}$ where $d(Mo\text{-}Mo)_{inter}$ and $d(Mo\text{-}Mo)_{intra}$ are the shortest Mo-Mo distances between and within the Mo_3 clusters, respectively. Later, Haraguchi et al. [36, 37] have demonstrated that the effective magnetic moment (μ_{eff}) is correlated to λ that they rename parameter of clusterization. Thus, when λ is sufficiently greater than one, the system can be categorized as a localized spin model while when λ is close to one, a weak Mott regime close to a metallic state is envisaged. Although, in our case, the Mo_3 clusters did not form a 2D-Kagome lattice but a kind of "1D", we can see on figure 10 that the value μ_{eff} observed for $La_3Mo_4SiO_{14}$ fits well with those of previous studies when we plot μ_{eff} as a function of λ for the reduced Mo compounds containing magnet Mo_3 aggregates, know to date. Among all of these compounds, it is interesting to note that $LiZn_2Mo_3O_8$ has a magnetic moment of 1.39 μ_B, correspondent to constant of Curie C = 0.24, at temperatures greater than 96 K while at lower temperatures, the magnetic moment is reduced to 0.8 μ_B (C = 0.08). According to Sheckelton et al. in 2012 [10], the diminution of the moment arises from the creation of an exotic condensed valence-bond ground state by 2/3 of the paramagnetic spins. At 14 K, the plot of the thermal variation of the magnetic susceptibility as a function of the temperature of $La_3Mo_4SiO_{14}$ (Fig.

9) presents a maximum arising probably from the apparition of a short range magnetic ordering between the triangular Mo_3 clusters as previously observed in $Li_2InMo_3O_8$ that was the first reduced Mo oxide presenting a long range magnetic ordering between the triangular clusters. In solid-state metal cluster chemistry, long-range ordering between unpaired electron clusters was first observed in the $GaMo_4X_8$ (X = S, Se) compounds [38] made in our laboratory and based on tetrahedral Mo_4 clusters with 11 electrons and that present ferromagnetic or antiferromagnetic interactions. A little more lately, antiferromagnetic interactions between octahedral Nb_6 cluster clusters containing 15 electrons were clearly evidenced by ^{19}F NMR and EPR measurements in the $LuNb_6Cl_{18}$ and Nb_6F_{15} compounds [39, 40]. well as for the compound $NdMo_8O_{14}$ [41] containing Mo_8 clusters with 23 electrons.

The temperature dependence of the inverse of the molar magnetic susceptibility of $Ce_3Mo_4SiO_{14}$, $Pr_3Mo_4SiO_{14}$ and $Nd_3Mo_4SiO_{14}$ are presented in Fig. 11. The susceptibility data for the Ce, Pr and Nd analogues show strong temperature dependencies and could be fit to modified Curie-Weiss like behaviours in the temperature range 100 – 300K. A least squares fitting of the observed after subtracting the contribution of the Mo_3 clusters resulted in a C = 2.11 emu.K/mole, $\theta = -14.72$ K and $\chi_0 = 2.46\ 10^{-3}$, C = 4.74 emu.K/mole, $\theta = -31.9$ K and $\chi_0 = 2.52\ 10^{-3}$, and C = 4.65 emu.K/mole, $\theta = -27.7$ K and $\chi_0 = 3.01\ 10^{-3}$ for the Ce, Pr and Nd compounds, respectively. The observed effective magnetic moments ($\mu_{eff.}$ = 2.37 μ_B/Ce, 3.55 3.52 μ_B/Pr and 3.52 μ_B/Nd) are in good agreement with the theoretically values of 2.54, 3.58 and 3.62 μ_B expected from Hund's rule [42]. In the case of the Pr compound, although the low symmetry of the Pr^{3+} sites, we did not observe an almost constant susceptibility below 10 K, indicating a non-magnetic single ground state as expected from the non-Kramer nature of the Pr^{3+} ions ($^3H_4$ ground state).

3. Conclusion

In summary, we have showed that the $Ln_3Mo_{4+x}Si_{1-x}O_{14}$ (Ln = La, Ce, Pr, and Nd; x = 0 and 0.33) compounds can be synthesized by solid state chemistry and, crystallize in the monoclinic space group $P2_1/n$ contrary to the $La_3Mo_4XO_{14}$ (x = Si or $Mo_{0.33}Al_{0.67}$) compounds prepared by electrolytic reduction at 1373 K of melts containing Na_2MoO_4, MoO_3, and La_2O_3 in silica or alumina crucibles which crystallize in the orthorhombic space group Pbam. The lowering of the space-group symmetry supresses the disordering of the Mo atoms forming the rutile-type Mo_2-chains. An electrical semi-conducting behaviour as previously found for the orthorhombic phases was also observed for $Pr_3Mo_{4.35}Si_{0.65}O_{14}$. Magnetic susceptibility measurements as a function of the temperature show a paramagnetic spin behaviour that confirm the presence of one unpaired electron per Mo_3 as expected from value of 7 e^-/Mo_3 and 4 e^-/Mo_2 deduced from the empirical bond length-bond strength relationship. Finally, the temperature dependence of the magnetic susceptibility shows a maximum at 14 K arising probably from an antiferromagnetic ordering between the Mo_3 clusters.

References

[1] W.H. McCarroll, L. Katz, R. Ward, Some Ternary Oxides Of Tetravalent Molybdenum. J. Am. Chem. Soc. 79 (1957) 5410–5414.

[2] Lijie Wen , Jing Zhai, Jianzheng Song , Hongping Jiang , Rui Cui , Yuanhui Xu, Keju Sun , Xianfeng Hao. Electronic and magnetic properties of polar magnets M2Mo3O8 (M = Mn, Fe, Co and Ni) from first principles studies. Journal of Solid State Chemistry 308 (2022) 122910

[3] T. Kurumaji, Y. Takahashi, J. Fujioka, R. Masuda, H. Shishikura, S. Ishiwata, Y. Tokura Electromagnon resonance in a collinear spin state of a polar antiferromagnet $Fe_2Mo_3O_8$, Phys. Rev. Lett. 119 (2017), 077207.

[4] T. Kurumaji, S. Ishiwata, Y. Tokura, Doping-Tunable Ferrimagnetic Phase with Large Linear Magnetoelectric Effect in a Polar Magnet $Fe_2Mo_3O_8$, Phys. Rev. X 5 (2015), 031034.

[5] S. Yu, B. Gao, J.W. Kim, S.-W. Cheong, M.K.L. Man, J. Madéo, K.M. Dani, D. Talbayev, High-temperature terahertz optical diode effect without magnetic order in polar FeZnMo3O8. Phys. Rev. Lett. 120 (2018), 037601.

[6] Y. Wang, G.L. Pascut, B. Gao, T.A. Tyson, K. Haule, V. Kiryukhin, S.-W. Cheong, Unveiling hidden ferrimagnetism and giant magnetoelectricity in polar magnet $Fe_2Mo_3O_8$. Sci. Rep. 5 (2015) 12268.

[7] Ideue, T., Kurumaji, T., Ishiwata, S. & Tokura, Y. Giant thermal Hall effect in multiferroics. Nat. Mater. 16, 797–802 (2017).

[8] Yongming Sun, Xianluo Hu, Wei Luo, Jie Shub and Yunhui Huang Self-assembly of hybrid $Fe_2Mo_3O_8$–reduced graphene oxide nanosheets with enhanced lithium storage properties. J. Mater. Chem. A, 2013,1, 4468-4474

[9] Hussen Maseed, Shaikshavali Petnikota, Vadali V. S. S. Srikanth, Madhavi Srinivasan, Chowdari B. V. R., M. V. Reddy and Stefan Adams, $Fe_2Mo_3O_8$/exfoliated graphene oxide: solid-state synthesis, characterization and anodic application in Li-ion batteries. New J. Chem., 2018,42, 12817-12823

[10] J. P. Sheckelton, J. R. Neilson, D. G. Soltan, T. M. McQueen, Possible valence-bond condensation in the frustrated cluster magnet $LiZn_2Mo_3O_8$. Nature Mat. 11 (2012) 493-496.

[11] J. P. Sheckelton, F. R. Foronda, LiDong Pan, C. Moir, R. D. McDonald, T. Lancaster, P. J. Baker, N. P. Armitage, T. Imai, S. J. Blundell, and T. M. McQueen, Local magnetism and spin correlations in the geometrically frustrated cluster magnet LiZn2Mo3O8. Phys. Rev. B 89, 064407 – Published 11 February 2014

[12] M. Mourigal, W. T. Fuhrman, J. P. Sheckelton, A. Wartelle, J. A. Rodriguez-Rivera, D. L. Abernathy, T. M. McQueen, and C. L. Broholm. Molecular Quantum Magnetism in LiZn2Mo3O8. Phys. Rev. Lett. 112, 027202 – Published 15 January 2014

[13] John P. Sheckelton, James R. Neilson and Tyrel M. McQueen. Electronic tunability of the frustrated triangular-lattice cluster magnet LiZn2-xMo3O8. Mater. Horiz., 2015, 2, 76.

[14] R. W. Betteridge, A. K. Cheetham, J. A. K. Howard, G. Jakubicki, W. H. McCarroll, Preparation and Crystal-Structure of $La_3Mo_4SiO_{14}$, An Unusual Cluster Compound of Molybdenum. Inorg. Chem. 23 (1984) 737-740.

[15] W. H. McCarroll, K. Podejko, A. K. Cheetham, D. M. Thomas, F. J. DiSalvo, The Crystal-Structure of $La_3Mo_{4.33}Al_{0.67}O_{14}$ and The Electronic-Structure of $La_3Mo_4XO_{14}$ (X = Si - $Mo_{1/3}Al_{2/3}$ - $Al_{1/2}V_{1/2}$). J. Solid State Chem. 62 (1986) 241-252.

[16] V. Petříček, M. Dušek, Jana2006—The Crystallographic Computing System, Institute of Physics, Praha, Czech Republic, 2006.

[17] Nonius BV, COLLECT, Data Collection Software, Nonius BV, 1999.

[18] A. J. M. Duisenberg, Reflections on area detectors, Ph.D. Thesis, Utrecht, 1998.

[19] J. de Meulenaar, H. Tompa, The Absorption Correction in Crystal Structure Analysis., Acta Crystallogr., Sect. A: Found. Crystallogr. 19 (1965) 1014.

[20] A. Altomare, M. C. Burla, M. Camalli, G. L. Cascarano, C. Giacovazzo, A. Guagliardi, A. G. G. Moliterni, G. Polidori, R. Spagna, SIR97: a new tool for crystal structure determination and refinement, J. Appl. Cryst. 32 (1999) 115.

[21] G. M. Sheldrick, SHELXL97, Program for the Refinement of Crystal Structures, University of Göttingen, Germany, 1997.

[22] A. L. Spek, Structure validation in chemical crystallography. Acta Cryst. D65 (2009) 148-155.

[23] B. J. Brandt, A. C. Skapski, A Refinement of Crystal Structure of Molybdenum Dioxide. Acta Chem. Scand. 21 (1967) 661.

[24] I.D. Brown and K.K. Wu, Empirical Parameters for Calculating Cation-Oxygen Bond Valences. Acta Crystallogr. B32 (1976) 1957-1959.

[25] J. Cuny, P. Gougeon, P. Gall, Redetermination of $Zn_2Mo_3O_8$. Acta Crystallogr. E65 (2009) I51.

[26] H. Abe, A. Sato, N. Tsujii, T. Furubayashi, M. Shimoda, Structural refinement of $T_2Mo_3O_8$ (T=Mg, Co, Zn and Mn) and anomalous valence of trinuclear molybdenum clusters in $Mn_2Mo_3O_8$. Journal of Solid State Chemistry 183 (2010) 379–384.

[27] P. Gall, P. Gougeon, $La_5Mo_6O_{21}$: a novel ternary reduced molybdenum oxide containing Mo^{IV}_3 clusters and isolated Mo^{V} centres. Acta Crystallographica Section C-Crystal Structure Communications 61 (2005) I69-I70.

[28] B.T. Collins, S.M. Fine, J.A. Potenza, P.-P. Tsai, M. Greenblatt, Crystallographic and magnetic studies of an unusual Mo_3O_{13} cluster compound, $Na_2In_2Mo_5O_{16}$. Inorganic Chemistry (1989) 28, p2444-p2447.

[29] K.G. Bramnik, E. Muessig, and H. Ehrenberg, Preparation, crystal structure, and magnetic studies of $Na_3Fe_2Mo_5O_{16}$, a new oxide containing Mo_3O_{13} clusters. Journal of Solid State Chemistry 176 (2003) 192–197.

[30] C. C. Torardi, R. E. McCarley, synthesis, crystal-structures, and properties of $LiZn_2Mo_3O_8$, $Zn_3Mo_3O_8$, and $ScZnMo_3O_8$, reduced derivatives containing the Mo_3O_{13} Cluster Unit. Inorg. Chem. 24 (1985) 476-481.

[31] P. Gall, R. Al Rahal Al Orabi, T. Guizouarn and P. Gougeon, Synthesis, crystal structure and magnetic properties of $Li_2InMo_3O_8$: a novel reduced molybdenum oxide containing magnetic Mo_3 clusters. J. Solid State Chem. 208 (2013) 99-102.

[32] P. Gall, R. Al Rahal Al Orabi, T. Guizouarn, J. Cuny, B. Fontaine, R. Gautier, P. Gougeon, Synthesis, crystal and electronic structures and magnetic properties of $Li_2SnMo_3O_8$: A novel reduced molybdenum oxide containing Mo_3O_{13} cluster units. J. of Solid State Chem. 201 (2013) 312–316.

[33] P. Gall, P. Gougeon, $Li_2GeMo_3O_8$: a novel reduced molybdenum oxide containing Mo3O13 cluster units, Acta Crystallographica Section E-Crystallographic Communications 72 (2016) 995-996.

[34] R.D. Shannon, Acta Crystallogr. A32 (1976) 751-767.

[35] G. Chen, H.-Y. Kee, and Y. B. Kim, Cluster Mott insulators and two Curie-Weiss regimes on an anisotropic kagome lattice, Phys. Rev. B, 93, 24, 245134

[36] Y. Haraguchi, C. Michioka, H. Ueda, K. Yoshimura, Highly Spin-Frustrated Magnetism in the Topochemically Prepared Triangular Lattice Cluster Magnets $Na_3A_2(MoO_4)_2Mo_3O_8$ (A=In, Sc). Chem. Eur. J. 23 (2017) 15879-15883.

[37] Haraguchi, Y.; Michioka, C.; Imai, M.; Ueda, H.; Yoshimura, K.Spin-liquid behavior in the spin-frustrated Mo_3 cluster magnet $Li_2ScMo_3O_8$ in contrast to magnetic ordering in isomorphic $Li_2InMo_3O_8$. Phys. Rev. B: Condens. Matter Mater. Phys.2015,92,014409.(11)

[38] H. Ben Yaich, J. C. Jegaden, M. Potel, R. Chevrel, M. Sergent, A. Berton, J. Chaussy, A. K. Rastogi, R. Tournier, $GaMo_4(XX')_8$ (X=S, Se, Te) new mixed chalcogenides with Mo_4 tetrahedral clusters. J. of Solid State Chem. 51 (1983) 212-217.

[39] S. Ihmaïne, C. Perrin, O. Pena, M. Sergent, Structure and magnetic-properties of 2 niobium chlorides with $(Nb_6Cl_{12})^{N+}$ (N=2, 3) units - $KLuNb_6Cl_{18}$ and $LuNb_6Cl_{18}$. J. Less-Common Met. 137 (1988) 323 –332.

[40] R. Knoll, J. Sokolovski, Y. BenHaim, A. I. Shames, S. D. Goren, H. Shaked, J.-Y. Thépot, C. Perrin, S. Cordier, Magnetic resonance and structural study of the cluster fluoride Nb_6F_{15}. Physica B 381 (2006) 47–52.

[41] R. Gautier, O. Krogh Andersen, P. Gougeon, J.-F. Halet, E. Canadell, J. D. Martin, Electronic structure, electrical and magnetic properties of RMo_8O_{14} compounds (R = La, Ce, Pr, Nd, Sm) containing bicapped Mo_8 clusters. Inorg. Chem. 41 (2002) 4689-4699.

[42] J. H. Van Vleck, Electric and Magnetic Susceptibilities, Oxford University Press, New York, 1932, p. 243.

Table Captions:

Table 1. Unit cell parameters of the $Ln_3Mo_4SiO_{14}$ compounds determined by profile matching fits.

Table 2. Crystal data and structure refinement for $Pr_3Mo_4(Mo_{0.35}Si_{0.65})O_{14}$.

Table 3. Selected Interatomic Distances for $Pr_3Mo_4(Mo_{0.35}Si_{0.65})O_{14}$.

Table 4**.** Number of electrons per Mo_3 cluster deduced from stoichiometry and from the Brown and Wu relationship for the compounds containing Mo_3 clusters.

Table 5. Effective magnetic moment for the compounds containing Mo_3 clusters with 7 electrons.

Figure Captions

Figure 1. Observed (dotted line), calculated (red line) and difference profiles for the refinement of $Pr_3Mo_4SiO_{14}$ in profile-matching mode (λ = 1.5406 Å).

Figure 2. Detail of the RX diagram of $Pr_3Mo_4SiO_{14}$ showing the lowering the unit-cell symmetry.

Figure 3. Variation of the unit cell volume for the monoclinic $Ln_3Mo_4SiO_{14}$ (Ln = La to Nd) compounds as a function of the Ln^{3+} ionic radius in eight coordination.

Figure 4. The crystal structure of $Pr_3Mo_4SiO_{14}$ as viewed down the a axis, parallel to the direction of the Mo_3O_{13} and MoO_6 chain growth. Ellipsoids are drawn at the 97 % probability level.

Figure 5. View of the Mo_3O_{13} cluster (ellipsoids at the 97 % probability level).

Figure 6. Fragment of the MoO_2-type chain.

Figure 7. Oxygen environments for the Pr atoms (ellipsoids at the 97 % probability level).

Figure 8.

Figure 9. Temperature dependence of the inverse magnetic susceptibility for $La_3Mo_4SiO_{14}$.

Figure 10. Plot of μ_{eff} as a function of the parameter $\lambda = d(Mo\text{-}Mo)_{inter}/d(Mo\text{-}Mo)_{intra}$

Figure 11. Reciprocal magnetic susceptibility of the $Ln_3Mo_4SiO_{14}$ (Ln = Ce, Pr, and Nd) compounds as a function of temperature. Data were taken under an applied field of 0.1 T.

	a (Å)	b (Å)	c (Å)	β (°)	Vol(Å^3)
$La_3Mo_4SiO_{14}$	5.6383(1)	17.6818(3)	11.0456(2)	90.2810(7)	1101.19(6)
$Ce_3Mo_4SiO_{14}$	5.6269(3)	17.6095(9)	10.9728(5)	90.2759(15)	1087.24(16)
$Pr_3Mo_4SiO_{14}$	5.6185(1)	17.5598(2)	10.9201(2)	90.3118(6)	1077.36(4)
$Nd_3Mo_4SiO_{14}$	5.6107(1)	17.5281(1)	10.8635(1)	90.3015(4)	1068.37(2)

Table 1. Unit cell parameters of the $Ln_3Mo_4SiO_{14}$ compounds determined by profile matching fits.

Table 2. Crystal data and structure refinements of $Pr_3Mo_4(Mo_{0.35}Si_{0.65})O_{14}$

Empirical formula	$Pr_3Mo_4(Mo_{0.348(4)}Si_{0.652(4)})O_{14}$
Formula weight ($gmol^{-1}$)	1081.65
Crystal system, space group	monoclinic, $P2_1/n$
Unit cell dimensions (Å, deg)	a = 5.6361 (2) b = 17.5814 (8) c = 10.9883 (4) β = 90.1654 (15)
Volume ($Å^3$)	1088.83 (7)
Z, Calculated density (g/cm^3)	4, 6.659
Absorption coefficient (mm−1)	18.140
Crystal color and habit	Black, needle like
Crystal size (mm^3)	0.181 × 0.034 × 0.025
Theta range for data collection (deg)	3.61–40.00
Limiting indices	$-10\leq h\leq 10$, $-25\leq k\leq 31$, $-19\leq l\leq 19$
Reflections collected/unique	36566/6749
R (int)	0.0454
Absorption correction	analytical
Max./min. transmission	0.6709/0.2026
Data/restraints/parameters	6749/0/202
Goodness-of-fit on F^2	1.121
R indices [$I>2\sigma(I)$]	R1=0.0302, wR2=0.0672
Extinction coefficient	0.00036(5)
Largest diff. peak and hole ($eÅ^{-3}$)	3.716 and −3.663

Table 3. Selected Interatomic Distances for $Pr_3Mo_4(Mo_{0.35}Si_{0.65})O_{14}$.

Mo(1)-Mo(3)	2.5400(6)	Mo(3)-O(10)	1.981(4)
Mo(1)-Mo(2)	2.5455(6)	Mo(3)-O(4)	2.011(4)
Mo(2)-Mo(3)	2.5584(4)	Mo(3)-O(2)	2.020(4)
Mo(1)-O(5)	1.928(4)	Mo(3)-O(9)	2.064(4)
Mo(1)-O(7)	1.946(4)	Mo(3)-O(1)	2.085(4)
Mo(1)-O(2)	2.021(4)	Mo(3)-O(11)	2.108(5)
Mo(1)-O(3)	2.027(4)	Mo4-Mo4	2.5083(7)
Mo(1)-O(1)	2.048(3)	Mo4-Mo4	3.1609(7)
Mo(1)-O(6)	2.132(4)	Mo(4)-O(9)	1.918(3)
Mo(2)-O(10)	2.001(4)	Mo(4)-O(13)	2.033(5)
Mo(2)-O(3)	2.034(5)	Mo(4)-O(13)	2.035(4)
Mo(2)-O(4)	2.044(3)	Mo(4)-O(4)	2.055(3)
Mo(2)-O(1)	2.083(4)	Mo(4)-O(12)	2.081(4)
Mo(2)-O(8)	2.085(6)	Mo(4)-O(12)	2.107(4)
Mo(2)-O(9)	2.094(4)		
Pr(1)-O(7)	2.334(5)	Pr(3)-O(7)	2.406(4)
Pr(1)-O(5)	2.358(5)	Pr(3)-O(13)	2.411(4)
Pr(1)-O(10)	2.454(3)	Pr(3)-O(12)	2.469(5)
Pr(1)-O(13)	2.473(4)	Pr(3)-O(8)	2.482(4)
Pr(1)-O(3)	2.529(4)	Pr(3)-O(11)	2.510(5)
Pr(1)-O(2)	2.546(4)	Pr(3)-O(5)	2.543(4)
Pr(1)-O(12)	2.569(4)	Pr(3)-O(6)	2.684(5)
Pr(1)-O(4)	2.742(4)		
Pr(2)-O(14)	2.405(5)	Si/Mo5-O14	1.460(5)
Pr(2)-O(2)	2.496(4)	Si/Mo5-O6	1.724(4)
Pr(2)-O(3)	2.504(4)	Si/Mo5-O11	1.741(5)
Pr(2)-O(5)	2.521(5)	Si/Mo5-O8	1.750(5)
Pr(2)-O(7)	2.571(5)		
Pr(2)-O(1)	2.578(3)		
Pr(2)-O(11)	2.761(6)		
Pr(2)-O(8)	2.775(6)		
Pr(2)-O(6)	2.802(6)		
Pr(2)-O(6)	2.936(6)		

Table 4**.** Number of electrons per Mo_3 cluster deduced from stoichiometry and from the Brown and Wu relationship as well as average or Mo-Mo distances (Å) in the Mo_3 clusters for compounds containing Mo_3 clusters the crystal structure of which was determined on single crystals.

		e^-/Mo_3 (stoichiometry)	e^-/Mo_3 (Brown and Wu)	Average or Mo-Mo distance (in Å) in the Mo_3 clusters	Space group	Reference
$Zn_2Mo_3O_8$	Mo_3	6	5.8	2.5326(2)	$P6_3mc$	25
$Zn_2Mo_3O_8$	Mo_3	6	6.0	2.5325(6)	$P6_3mc$	26
$Mg_2Mo_3O_8$	Mo_3	6	5.8	2.5271(2)	$P6_3mc$	26
$Co_2Mo_3O_8$	Mo_3	6	5.8	2.5274(2)	$P6_3mc$	26
$Mn_2Mo_3O_8$	Mo_3	6	6.0	2.5391(6)	$P6_3mc$	26
$La_5Mo_6O_{21}$	$Mo_3 + Mo^{5+}$	6	6.3	2.5598(6)	$P2_12_12_1$	27
$Na_2In_2Mo_5O_{16}$	Mo_3+Mo^{6+}	6	6.3	2.6164(5)	P3m1	28
$La_3Mo_4Al_{2/3}Mo_{1/3}O_{14}$	Mo_3+Mo_2	6.33	6	2.568	Pnma	15
$La_3Mo_4SiO_{14}$	Mo_3+Mo_2	7	6.5	2.555	Pnma	14
$Na_3Fe_2Mo_5O_{16}$	Mo_3+Mo^{6+}	7	6.5	2.567(1)	P-3m1	29
$Pr_3Mo_4(Mo_{0.35}Si_{0.65})O_{14}$	Mo_3+Mo_2	7	6.8	2.548	$P2_1/n$	This study
$LiZn_2Mo_3O_8$	Mo_3	7	7.4	2.578(1)	R-3m	30
$Li_2InMo_3O_8$	Mo_3	7	7.4	2.5455(4)	$P6_3mc$	31
$Li_2SnMo_3O_8$	Mo_3	8	8	2.5036(7)	$P6_3mc$	32
$Li_2GeMo_3O_8$	Mo_3	8	7.9	2.4728(8)	$P6_3mc$	33
$Zn_3Mo_3O_8$	Mo_3	8	8.3	2.580(2)	R-3m	30

Table 5. Effective magnetic moment for the compounds containing Mo_3 clusters with 7 electrons and non-magnetic cations.

	μeff (μB)	Reference
$La_3Mo_4SiO_{14}$	1.41	This work
$LiZn_2Mo_3O_8$	1.39 (T>96 K)	20
$LiZn_2Mo_3O_8$	1.2	15
$ScZnMo_3O_8$	1.50	15
$Li_2InMo_3O_8$	1.50	16
$Li_2ScMo_3O_8$	1.65	22
$Na_3In_2(MoO_4)_2Mo_3O_8$	1.43	21
$Na_3Sc_2(MoO_4)_2Mo_3O_8$	1.46	21
$Na_2In_2(MoO_4)_2Mo_3O_8$	0.366	21
$Na_2Sc_2(MoO_4)_2Mo_3O_8$	0.340	21

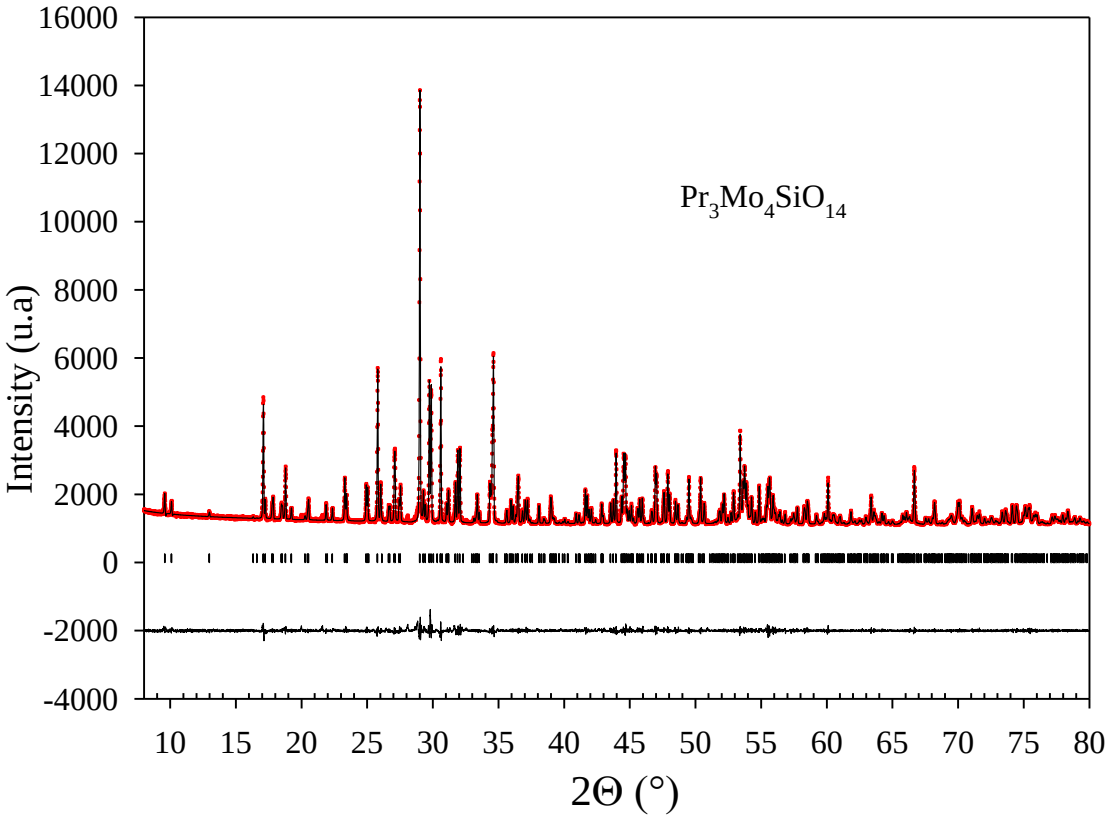
16000
14000
12000
10000
8000
6000
4000
2000
0
-2000
-4000
Intensity (u.a)
Pr3Mo4SiO14
10
15
20
25
30
35
40
45
50
55
60
65
70
75
80
2Θ (°)

Figure 1

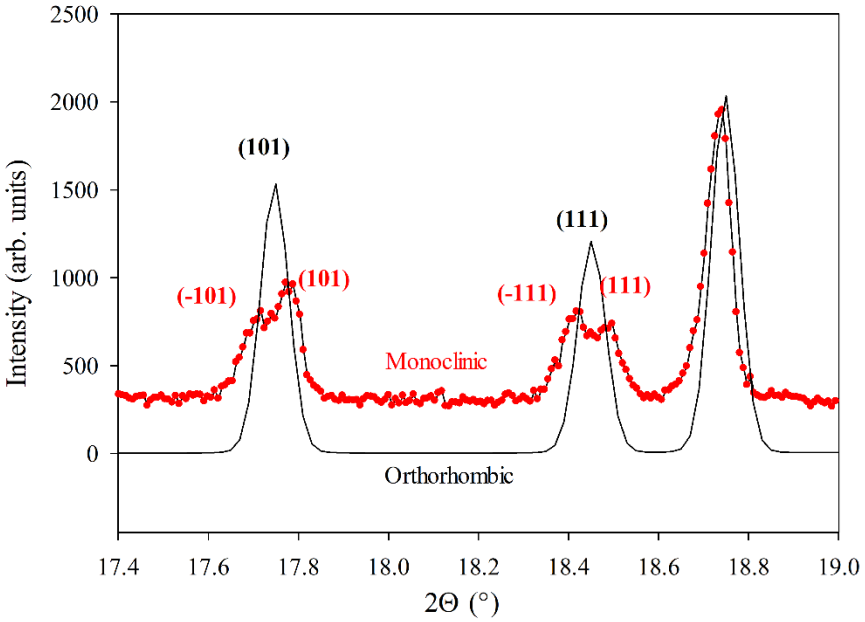
2500
2000
1500
1000
500
0
Intensity (arb. units)
(101)
(-101)
(101)
(111)
(-111)
(111)
Monoclinic
Orthorhombic
17.4
17.6
17.8
18.0
18.2
18.4
18.6
18.8
19.0
2Θ (°)

Figure 2

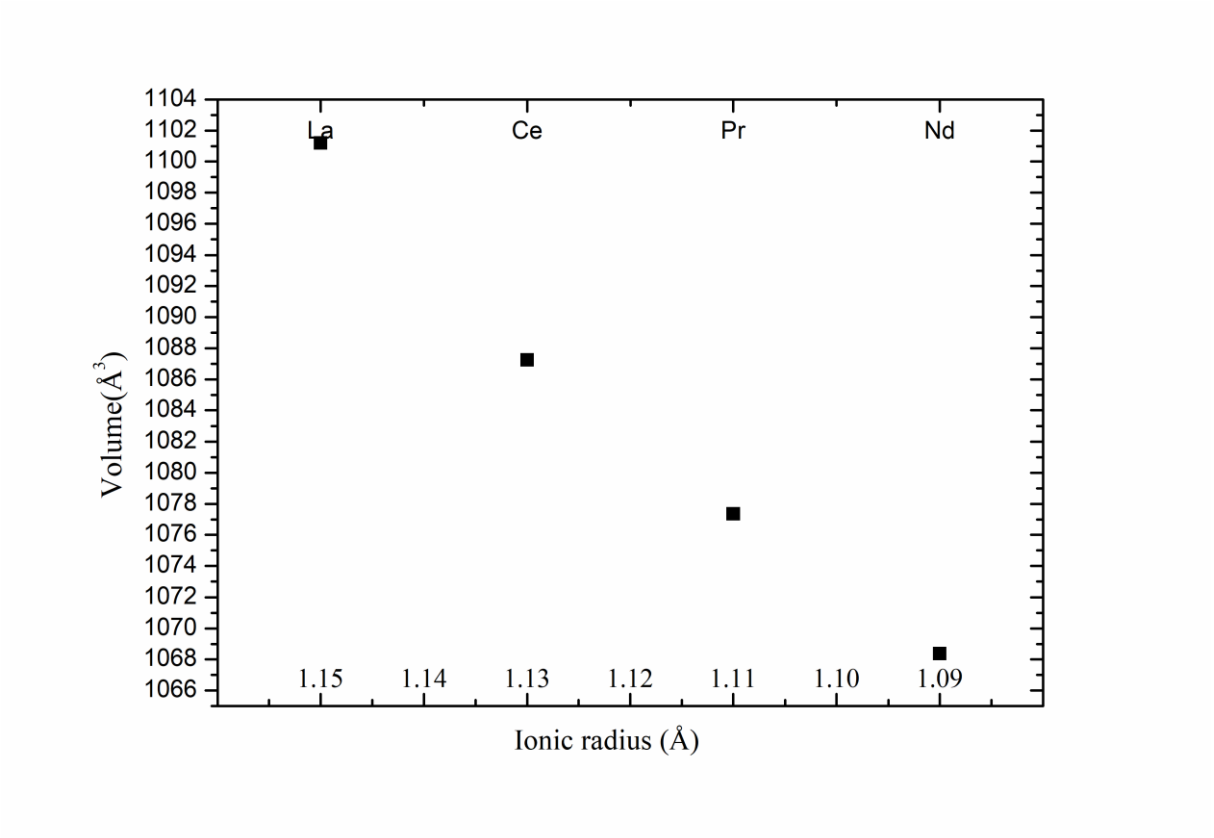

Figure 3. Variation of the unit cell volume for the monoclinic $Ln_3Mo_4SiO_{14}$ (Ln = La to Nd) compounds as a function of the Ln^{3+} ionic radius in eight coordination.

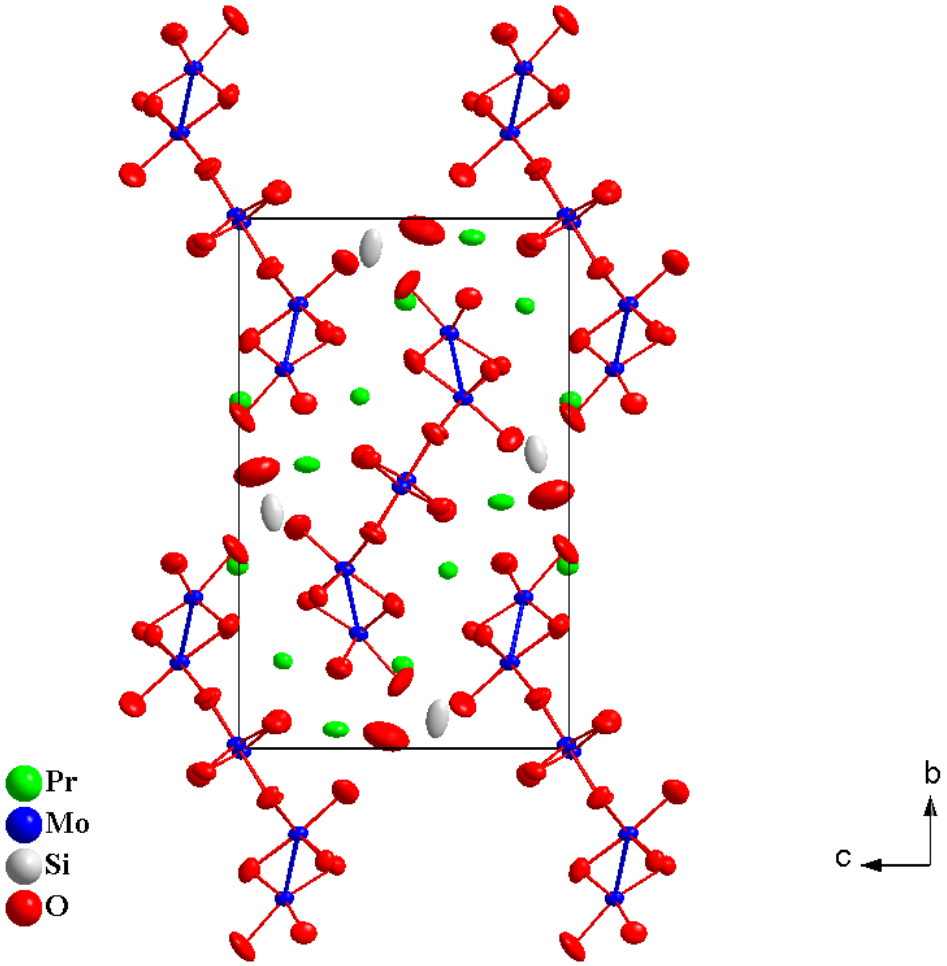

Figure 4

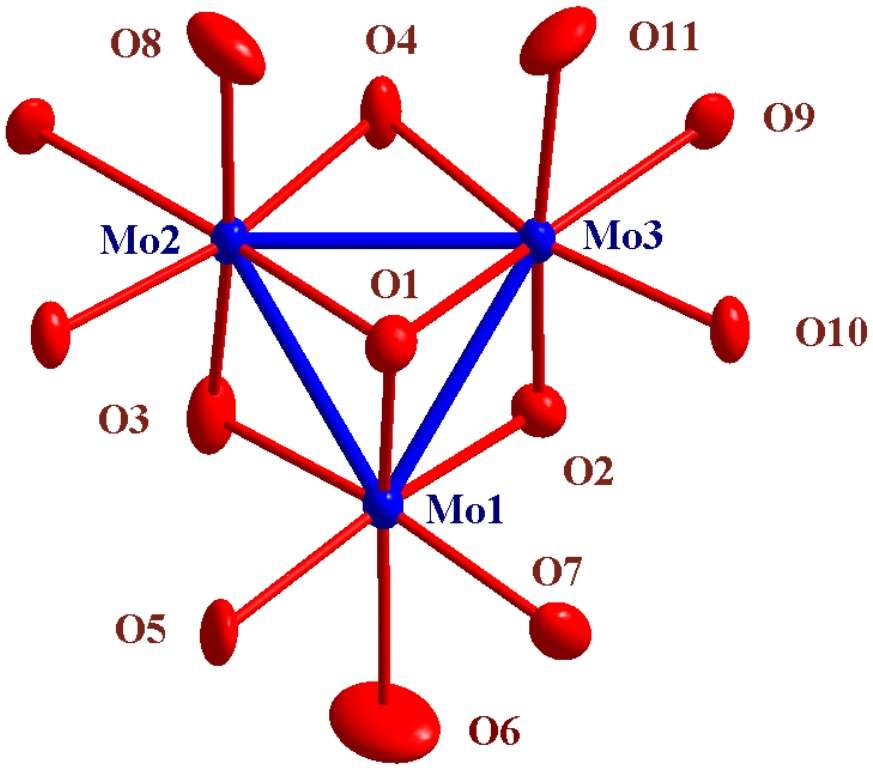

Figure 5

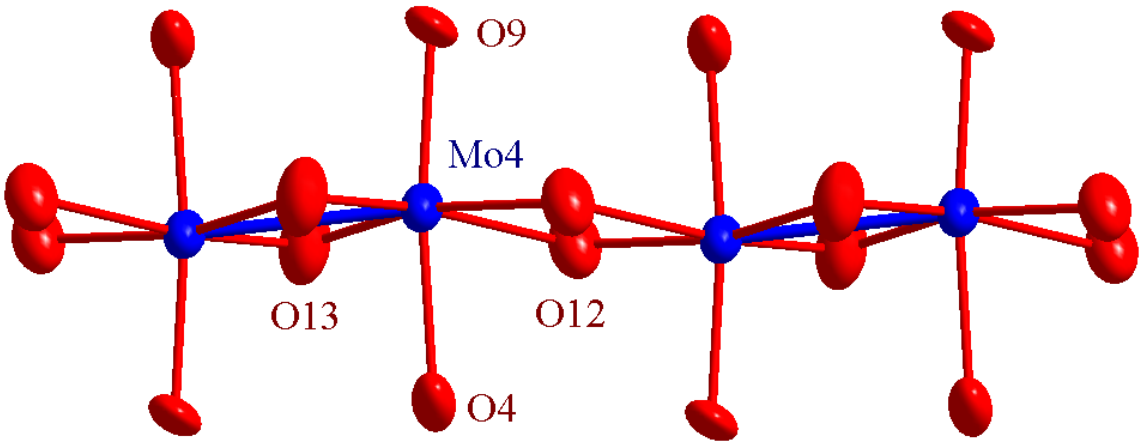

Figure 6

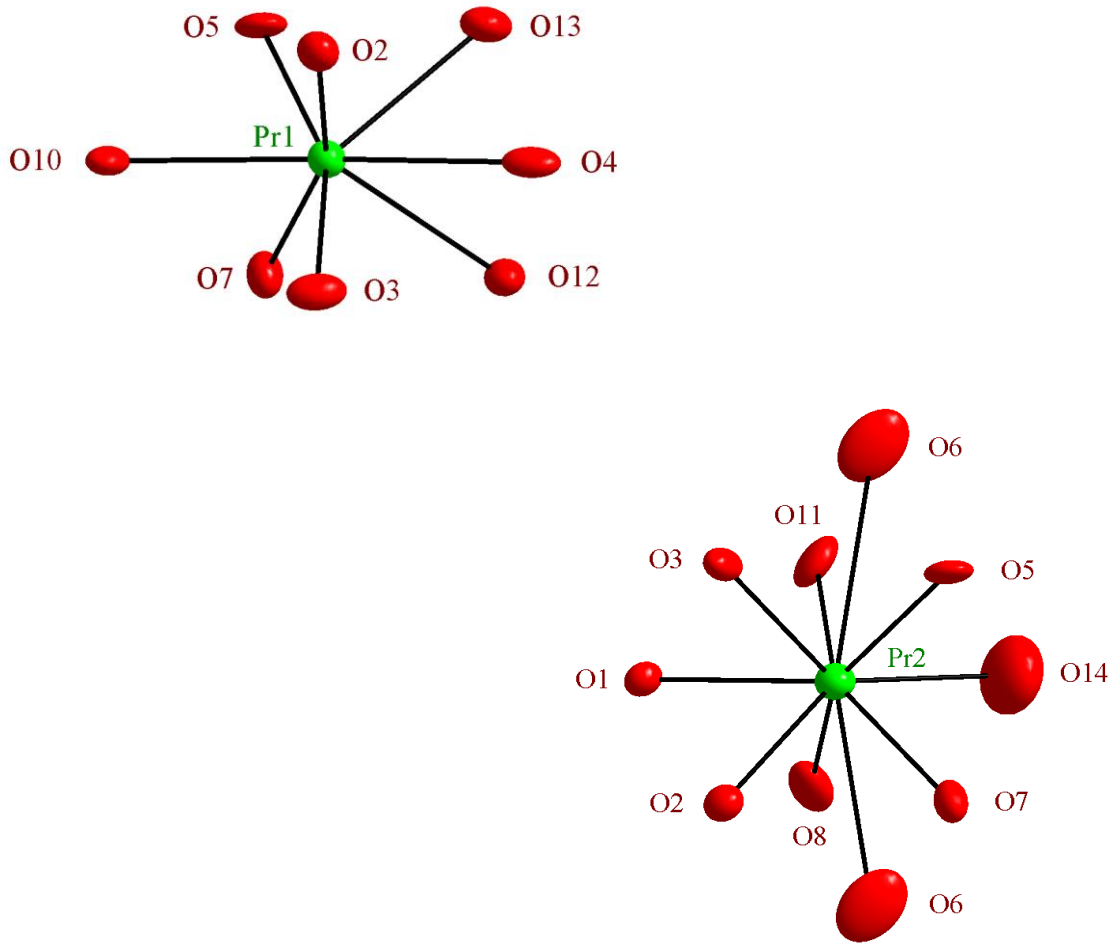
O5
O2
O13
Pr1
O10
O4
O7
O3
O12
O6
O11
O3
O5
Pr2
O1
O14
O2
O8
O7
O6
O12
O7
O8
Pr3
O6
O13
O11
O5

Figure 7

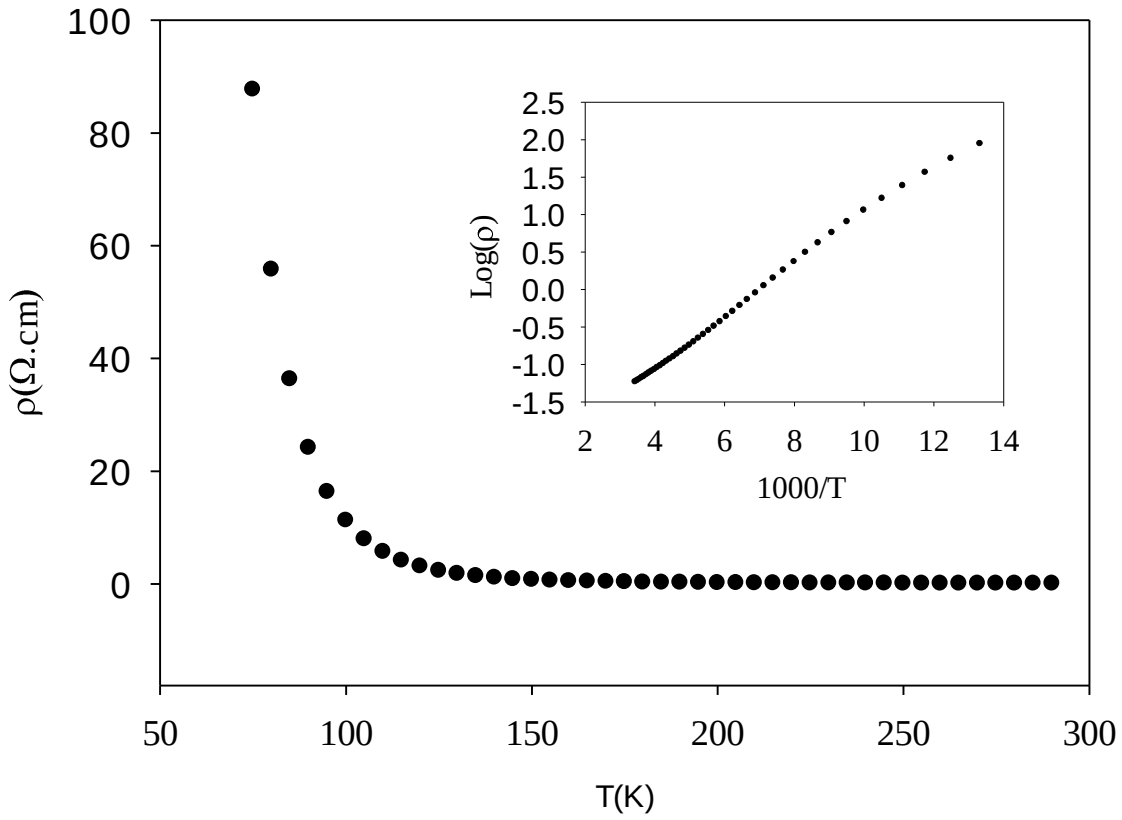
100
80
60
40
20
0
ρ(Ω.cm)
50
100
150
200
250
300
T(K)
2.5
2.0
1.5
1.0
0.5
0.0
-0.5
-1.0
-1.5
Log(ρ)
2
4
6
8
10
12
14
1000/T

Figure 8

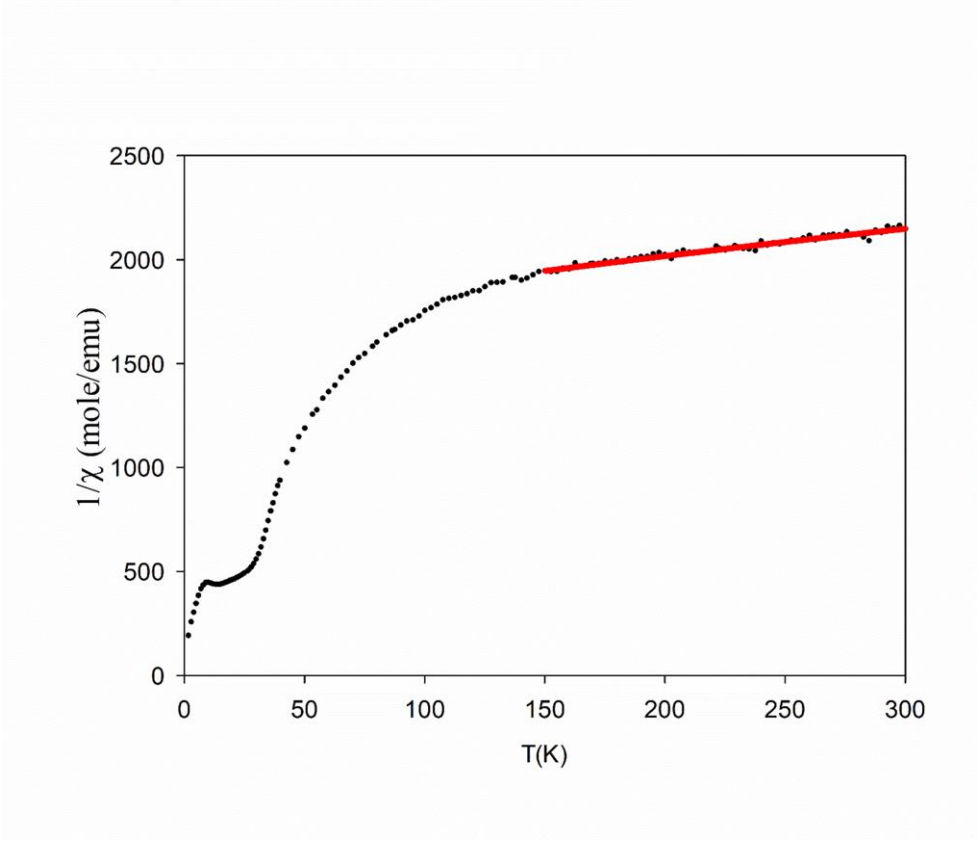

Figure 9

Figure 10

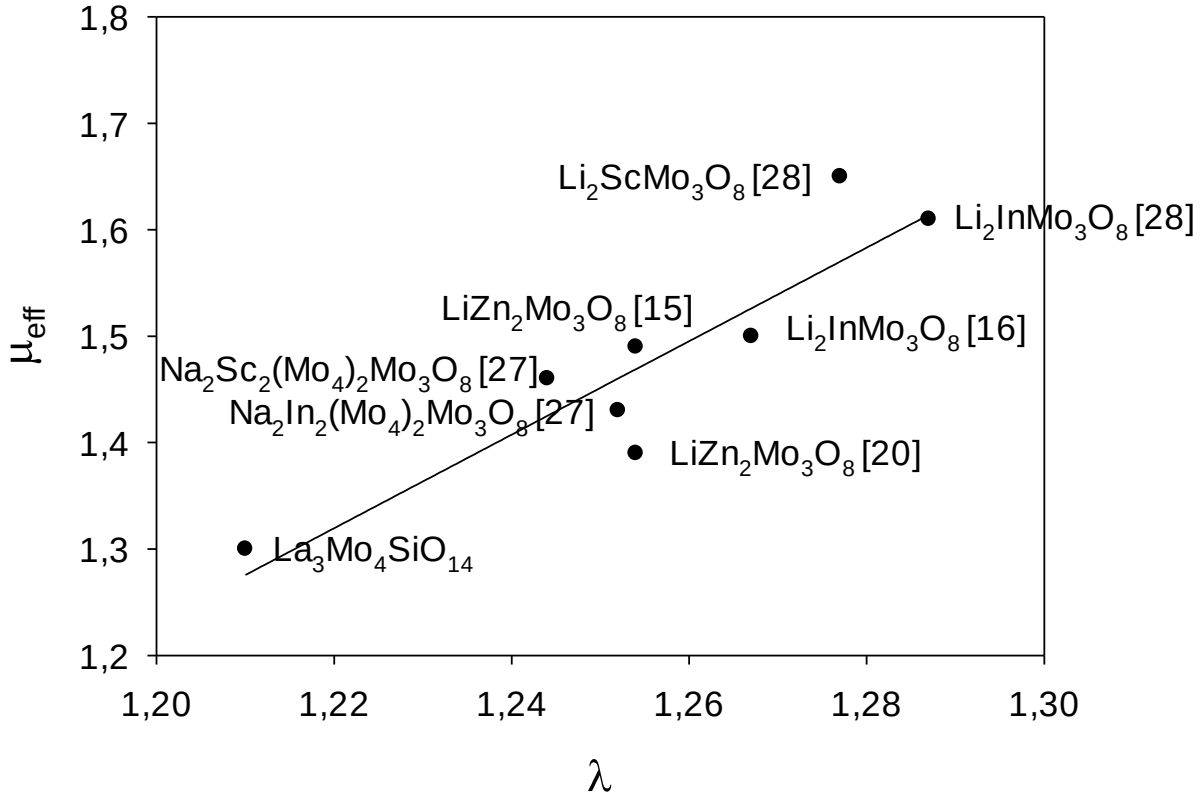
1,8
1,7
1,6
1,5
1,4
1,3
1,2
μeff
1,20
1,22
1,24
1,26
1,28
1,30
λ
Li2ScMo3O8 [28]
Li2InMo3O8 [28]
LiZn2Mo3O8 [15]
Li2InMo3O8 [16]
Na2Sc2(Mo4)2Mo3O8 [27]
Na2In2(Mo4)2Mo3O8 [27]
LiZn2Mo3O8 [20]
La3Mo4SiO14

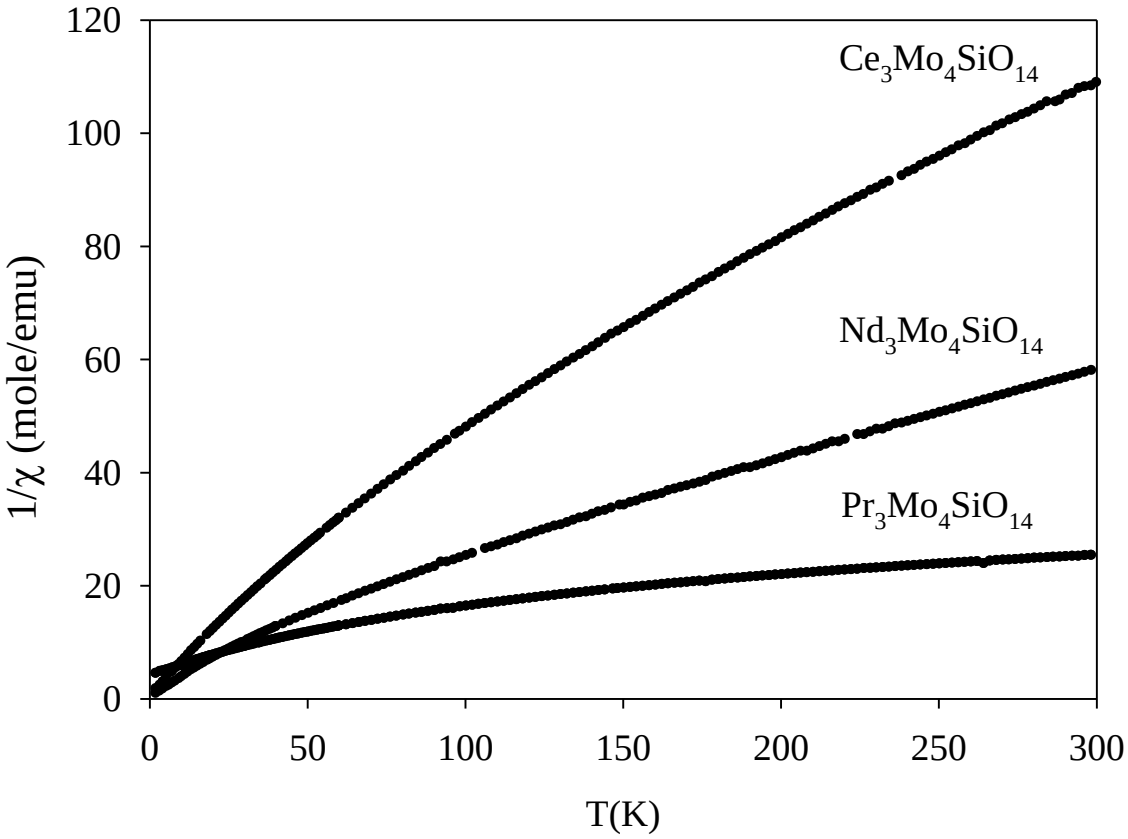
120
100
80
60
40
20
0
1/χ (mole/emu)
0
50
100
150
200
250
300
T(K)
Ce3Mo4SiO14
Nd3Mo4SiO14
Pr3Mo4SiO14

Figure 11